

Received 22 July 2023, accepted 29 July 2023, date of publication 1 August 2023, date of current version 9 August 2023.

Digital Object Identifier 10.1109/ACCESS.2023.3300960

## RESEARCH ARTICLE

# 5G Millimeter Wave Network Optimization: Dual Connectivity and Power Allocation Strategy

**ABDULHALIM FAYAD**<sup>1</sup>, (Graduate Student Member, IEEE), **TIBOR CINKLER**<sup>1,2,3</sup>,  
**AND JACEK RAK**<sup>3</sup>, (Senior Member, IEEE)

<sup>1</sup>Department of Telecommunications and Media Informatics, Budapest University of Technology and Economics, 1111 Budapest, Hungary

<sup>2</sup>ELKH-BME Cloud Applications Research Group, 1111 Budapest, Hungary

<sup>3</sup>Department of Computer Communications, Gdańsk University of Technology, 80-233 Gdańsk, Poland

Corresponding author: Abdulhalim Fayad (fayad@tmit.bme.hu)

This work was supported by CHIST-ERA Sustainable and Adaptive Ultra-High-Capacity Micro Base Stations (SAMBAS) Grant funded by Research Foundation–Flanders (FWO), Agence nationale de la Recherche (ANR), National Research, Development and Innovation Office (NKFIH), and UK Research and Innovation (UKRI), under Grant CHIST-ERA-20-SICT-003.

**ABSTRACT** The fifth generation (5G) of mobile networks utilizing millimeter Wave (mmWave) bands can be considered the leading player in meeting the continuously increasing hunger of the end user demands in the near future. However, 5G networks are characterized by high power consumption, which poses a significant challenge to the efficient management of base stations (BSs) and user association. Implementing new power consumption and user association strategies is imperative to address this issue. For that in this work, we focus on the Dual Connectivity-User and Power Allocation (DC-UPA) problem utilizing BS switching on/off along with user dual connectivity. The problem is mathematically formulated as an Integer Linear Program (ILP), and its NP-hardness is proven by showing its equivalence to a variant of the set covering problem. Moreover, we developed two heuristic algorithms: Simulated Annealing (SA) and Distance-Aware (DA) greedy, to mitigate the impact of the problem complexity and resolve the ILP scalability issue. We conducted extensive simulations to validate the effectiveness of the proposed heuristics in a two-dimensional area containing multiple BSs and users with uniform and nonuniform geographical distributions. The performance of the SA and DA algorithms was compared against the ILP approach. We evaluated the performance of the proposed solutions considering different aspects such as the number of users, the BS radius, and the traffic load changes. The numerical results show that SA outperforms the DA in both uniform and nonuniform geographical distributions of users. The SA provides a sub-optimal solution with an optimality gap of about 3.2%, while the optimality gap of the DA is 8.62% in the case of the uniform distribution. Moreover, the optimality gap in the case of nonuniform distribution is equal to about 1% and 5.2% of SA and DA, respectively. Additionally, by utilizing our solutions, the reduction of the level of power consumption up to 16.1% and 20% in the case of uniform and nonuniform distributions can be achieved. The obtained results highlight the efficiency of the proposed algorithms in addressing the DC-UPA problem, providing practical solutions for managing power consumption and maintaining continuous user connectivity in 5G mmWave networks.

**INDEX TERMS** 5G, mmwave, power consumption, ILP, simulated annealing (SA), distance aware (DA), dual connectivity, optimization.

## I. INTRODUCTION

The proliferation of connected devices in recent years has resulted in a rapid increase in the number of mobile

The associate editor coordinating the review of this manuscript and approving it for publication was Mostafa M. Fouda<sup>1</sup>.

data traffic, with predictions estimating that by 2030, the overall global mobile data traffic will reach 5 zettabytes (ZB) ( $10^{21}$  Bytes) monthly, and individual data rates will reach 100 Gbps ( $10^{11}$  bps) [1], [2]. As a result, mobile network operators (MNOs) face the major challenge of meeting the steadily increasing demand for high data

rates. In response, the fifth-generation (5G) wireless mobile communication networks were deployed in 2020, offering users significant enhancements such as high data rates, low latency (<3 ms), improved capacity, and better quality of service (QoS) [3]. 5G networks are designed to support three main applications: enhanced mobile broadband (eMBB), ultra-reliable low latency communication (URLLC), and massive machine-type communication (mMTC) [3]. However, 5G technology may not be able to support the emerged applications in the near future that require data rates in the Tbps range, latency less than a few hundred microseconds, and connectivity surpassing tens of millions of connections per km<sup>2</sup> [4]. Therefore, despite ongoing 5G deployment on a global scale, academia and industry must already shift their focus towards the development to beyond 5G or sixth-generation (6G) systems. That is necessary to support new applications which require ultra-high-speed data transmissions, ultra-low latency, and ultra-reliable connectivity, such as augmented reality (AR), virtual reality (VR), holographic communications, and tactile internet anticipated by 2030 [5].

To support future 6G networks, enablers such as new spectrum bands e.g. millimeter wave (mmWave) and sub-THz, massive multiple-input multiple-output (MIMO) (higher than  $64 \times 64$ ), new beamforming techniques, and network densification are required [6]. Among them, the mmWave frequencies, offering high bandwidth and data rates are expected to become the major technology for beyond 5G as well as 6G wireless mobile communications [7], [8]. The term “mmWave” refers to the spectrum bands between 24 and 300 GHz [9]. However, signals of these frequencies have a shorter range, which requires more base stations (BSs) and higher transmission energy, leading to a need for high network densification [10]. The term “network densification” refers to deploying a dense network comprised of low-power small cells or small BSs.

New challenges have emerged due to the transition toward 5G and beyond and the need for denser mobile access networks. These include a notable rise in the overall power consumption and increased carbon dioxide (CO<sub>2</sub>) emissions from wireless networks, which impact carbon footprint.

The growing pollution caused by the extensive energy usage of 5G and beyond networks has become a significant concern for many experts and stakeholders, working towards finding sustainable solutions for minimizing the network carbon footprint. Information and communication technology (ICT) consumes 4.7% of the worldwide electrical energy and contributes 1.7% of the world’s CO<sub>2</sub> emissions to the atmosphere and around 3-4.5% of global toxic ejections worldwide [11].

Furthermore, as per [12], the telecommunications sector’s yearly energy usage is increasing and is predicted to constitute 51% of global electricity consumption in 2030 unless the wireless access networks’ energy efficiency is significantly enhanced. Hence, the energy consumption reduction over wireless networks has become an essential goal, for that it is critical to work on design of green

networking solutions that can handle the growing traffic demand without compromising user quality of service (QoS) while also preventing worst-case scenarios from occurring. This means they can avoid the serious energy consumption and the significant environmental impact caused by carbon footprint.

Additionally, it is crucial from the economic standpoint for MNOs as well because paying the electricity bill accounts for a large amount of their operating expenditures (Opex). Energy expenditures make around 20% to 40% of all network Opex, or about \$3 billion annually in the US and \$7 billion in Europe, where the price of electricity increased dramatically, according to [13]. Additionally, it is forecasted that by 2030, the total energy consumption in the ICT industry will be increased from 611 TWh to 1852 TWh [14].

### A. MOTIVATION

BSs in wireless networks are responsible for a large part of the energy consumption, which may reach up to 80% of the total energy consumption of wireless mobile networks, in some cases [15]. Numerous methods exist for attaining energy reduction in wireless networks [16]. BSs switching on/off (also called BS sleep control) is widely regarded as an effective approach for saving energy and enhancing energy efficiency [17]. This technique allows BSs to alternate between active and sleep modes to decrease power consumption during periods of low traffic demand, while still ensuring that the network coverage is maintained.

Furthermore, to maintain connectivity of users under different situations including failures, dual connectivity can be introduced as a solution for that [18], [19]. Connecting each user to two BSs instead of one can provide several benefits, including (1) Increased capacity: By connecting a user to two BSs, the user can utilize the combined capacity of both BSs. This results in increased capacity, which can improve the overall network performance and user experience. (2) Improved coverage: By connecting a user to two BSs, the user can benefit from improved coverage. This is especially true in areas with weak signals, where connecting to multiple BSs can help improve signal strength and reduce dropouts. (3) Enhanced resiliency/availability: By connecting a user to two BSs, the user can benefit from enhanced resiliency. If one BS experiences an outage or congestion, the user can still be served by the other BS, thereby minimizing the impact on the user experience. (4) Load balancing: The network can achieve better load balancing by connecting a user to two BSs. The network can dynamically allocate resources between the two BSs based on the user’s location, network conditions, and other factors.

An example about the BS switching on/off with dual connectivity is illustrated in Fig. 1. The figure illustrates the status of BSs in the network. We can observe that the green-colored BSs represent the inactive BSs (switched off), where there are no users allocated to any of those BSs. Moreover, the black-colored BSs represent the active

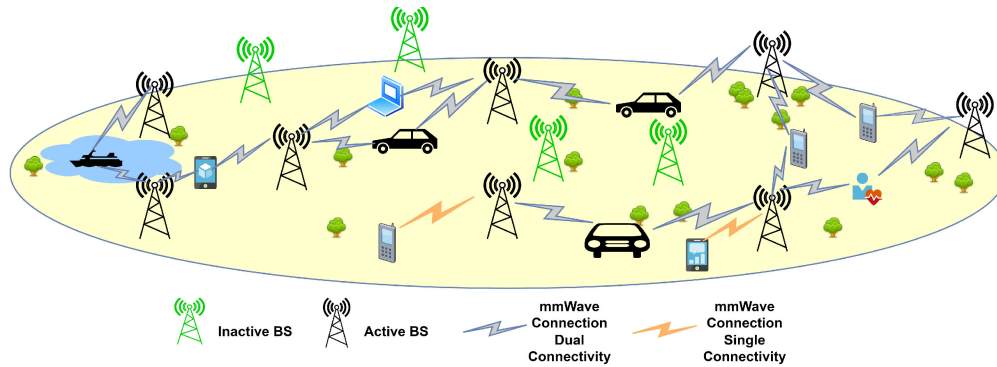


**FIGURE 1.** Example of the network deployment with BS switching on/off and dual connectivity.

BSs (switched on) in the network, where at least one user is assigned to each of those BSs. Additionally, the grey connections represent the dual connectivity for the end users, where each user is connected to two BSs simultaneously. In contrast, the orange link shows that the user is connected to one BS only (single connectivity).

### B. THE MAIN CONTRIBUTIONS

As previously stated and driven by the earlier considerations, the primary goal of this paper is to address the challenge of user association and power allocation with dual connectivity for 5G mmWave networks based on BS switching on/off strategies. The main contributions of our paper can be summarized as follows:

- 1) Firstly, the mathematical formulation of the DC-UPA problem for 5G mmWave networks as an Integer Linear Program (ILP) considering various constraints. The objective is to minimize the power consumption over switching on/off the network BSs while simultaneously connecting each user to two BSs if different constraints are satisfied (in the worst case, the user is allocated to one cell only).
- 2) Secondly, proving that the DC-UPA problem is an NP-hard one by formulating it as a variant of a set covering problem.
- 3) Thirdly, considering the complexity of the DC-UPA problem, we present two efficient heuristic algorithms: (1) Simulated Annealing (SA) and (2) Distance-Aware (DA) greedy algorithm.
- 4) Finally, conducting extensive simulations to validate the effectiveness of these proposed heuristics, a comparison of their performance with the ILP approach, applying the proposed solutions in two dimension area containing a number of BSs and a number of users with two different geographical user distributions (uniform and nonuniform).

### C. ORGANIZATION OF THE PAPER

The rest of the paper is organized as follows: Section II presents a comprehensive review of prior research and highlights the main contributions of our paper. In Section III,

the system modeling, problem formulation and the proposed solutions are elaborated. Specifically, Section III focuses on formulating the problem as an ILP and introduces two heuristic algorithms as potential solutions. Section IV discusses results of the extensive performance analysis of the proposed approaches and examines the obtained results. Finally, Section V summarizes the key findings and concludes the paper.

## II. PRIOR WORKS REVIEW

The widespread adoption of wireless communication technology has led to a surge in user traffic worldwide, resulting in a corresponding rise in energy consumption by the ICT sector, as more and more BSs are deployed to handle this increased demand. Consequently, there has been a significant push in the literature to focus on reducing energy consumption across wireless networks and developing energy-efficient network design strategies.

The authors of [20] proposed an algorithm to optimize energy efficiency in 5G wireless communications using millimeter-wave massive MIMO systems with ultra-dense heterogeneous networks. Likewise, the authors of [21] and [22] looked into the joint user association and power allocation-based energy efficiency maximization in heterogeneous networks.

A combinatorial framework that includes dynamic BS sleep/awake operation, adaptive resource block allocation, and enables an effective trade-off mechanism between system performance with traffic handling and energy consumption was proposed by the authors of [23] and [24].

The authors of [25] proposed a scheme that combines ultra-dense network and user-centric virtual cell architecture to improve the transmission performance of millimeter-wave communication in 5G wireless systems. The proposed scheme uses the coordinated multipoint (CoMP) transmission technology to mitigate interference and a dedicated algorithm to optimize user association and power allocation while satisfying QoS requirements.

In order to lower the energy usage in heterogeneous networks, the authors of [26] investigated BS on/off (awake/sleep) control techniques. Moreover, the authors

of [27] presented a joint optimization method for improving the energy efficiency of ultra-dense networks (UDNs) by considering user association and small BS on/off strategies. Similarly, the authors of [28] proposed a strategy to maximize network energy efficiency in 5G networks using dynamic femtocell gNB on/off strategies.

Additionally, the authors of [29] investigated energy consumption in 5G networks and proposed a solution using Cloud Radio Access Network (C-RAN) architecture, switching on/off cell sectors, and densification using Small Cell Remote Radio Heads (SC-RRHs).

Furthermore, the authors of [30] proposed access point (AP) switch on/off (ASO) strategies for green cell-free massive MIMO networks, which consist of a large number of distributed access points serving mobile stations. Likewise, the authors [31] presented a switching-on/off-based energy-saving algorithm for reducing energy consumption in wireless cellular networks.

The authors of [32] presented an approach to minimize the total power consumption of a heterogeneous cellular network (HCN) by jointly designing energy-efficient user association and small cell BSs switching on/off schemes. The authors of [33] proposed an intelligent BS sleeping scheme for 5G and beyond mobile communication systems, which reduces energy consumption by over 40% on average. The authors of [34] proposed the use of multi-connectivity-enabled user association (MCUA) to alleviate issues in ultra-dense mmWave networks. They jointly optimized MCUAs and downlink power allocations (PAs) to maximize the DL rate of each user, solving a complicated non-convex optimization problem using a weighted sum method and iterative algorithms.

Additionally, the authors of [35] addressed the challenge of reducing energy consumption in UDN by controlling the power-saving mode of small cell BSs, while ensuring network coverage and performance requirements. The proposed scheme optimizes BS selection for energy efficiency while considering QoS constraints. They considered uniform and non-uniform users distribution scenarios.

Moreover, to reduce energy consumption and improve connectivity in ultra-dense small cell networks, an efficient cell modeling algorithm (ECM) and binary particle swarm optimization-based small cell deployment (BPSD) were proposed in [36]. The proposed algorithm dynamically controls the sleep mode of BSs without compromising network performance, resulting in improved energy efficiency and connectivity. The authors of [37] discussed using mmWave technology UDNs to improve energy and spectral efficiency. They addressed the challenges of user association and power allocation in mmWave-based UDNs, considering that each user is allocated to one BS only.

Additionally, the authors of [38] examined the prospect of enhancing the resiliency of 5G networks as well as looked into reducing the power consumption through BSs switching-off strategy.

Finally, the authors of [39] presented hybrid beamformer designs for a multi-user multi-cell mmWave system. The designs minimize transmit power while ensuring QoS constraints at each mobile station. The paper introduces centralized and distributed approaches, extends them to handle imperfect channel state information (CSI), and demonstrates their performance through simulations.

However, to the best of our knowledge, the problem of user allocations with dual connectivity and power allocation in 5G mmWave networks has not been studied in prior studies. Table 1 shows a comparison of the contribution of our work with the prior research results available in the literature.

### III. SYSTEM MODEL AND PROBLEM FORMULATION

#### A. NETWORK MODEL

Considering a mmWave 5G network that consists of a set  $S$  of BSs,  $s \in \{1, \dots, S\}$ ,  $\forall s \in |S|$  are distributed uniformly in the two dimensional area. Each BS in the network has two possible states: active mode (on) and inactive mode (off), where, the active mode is used to transmit data to users, while the inactive mode is used to save energy when there is no data transmission. The set of User Equipment (UEs)  $u \in U \triangleq \{1, \dots, U\}$ ,  $\forall u \in |U|$  to communicate with the small cells, the set of users and be distributed in the area with uniform or nonuniform distribution. All BSs and UEs are equipped with a single omnidirectional antenna. We assume that each user can be assigned to two BSs at the same time. In this paper, we only consider the downlink communications scenario, i.e., from the BS to the UE. Additionally, we consider that all UEs are moving according to a random walk scenario (discussed in Section III-C).

The approximate daily traffic arrival seen in Fig. 2 can be estimated using the Poisson distribution model as in [42] as follows:

$$\lambda(t) = \frac{p(t, \alpha)}{\max[p(t, \alpha)]} \quad (1)$$

$$p(t, \alpha) = \frac{\alpha^t}{t!} e^{-\alpha} \quad (2)$$

where  $t$  represents the time,  $\lambda(t)$  represents the normalized traffic distribution,  $p(t, \alpha)$  represents the Poisson distribution function of traffic demand, and  $\alpha$  is the average value of peak number of traffic arrivals.

#### B. WIRELESS NETWORK DIMENSIONING

As our study focuses on the use of mmWave frequencies, we employ a path loss model that is known as Floating-Intercept Path Loss Model and can be used for mmWave bands [40]. The path loss model is given by:

$$L(d) = L(d_0) + \eta 10 \log_{10}(d) + \xi, \quad \xi \sim N(0, \sigma^2) \quad (3)$$

where

$$L(d_0) = 20 \log_{10} \left( \frac{4\pi d_0}{\lambda} \right) \quad (4)$$



TABLE 1. Our contribution in comparison to the related works.

Contributions	[20]	[21]	[22]	[23]	[24]	[25]	[26]	[27]	[28]	[29]	[30]	[31]	[32]	[33]	[34]	[35]	[36]	[37]	[38]	[39]	Our work
mmWave	✓	-	✓	-	-	✓	-	-	-	✓	-	-	-	✓	✓	-	✓	-	✓	✓	✓
Dual connectivity	-	-	-	-	-	-	-	-	✓	-	-	-	-	-	-	-	-	-	-	-	✓
User mobility	-	-	-	-	-	-	-	✓	-	-	-	-	-	-	-	-	-	-	-	-	✓
Different users distributions	-	-	-	-	-	-	-	-	-	-	-	-	-	-	-	✓	-	-	-	-	✓
Power and user allocation	✓	✓	✓	✓	✓	✓	✓	✓	✓	✓	✓	✓	✓	✓	✓	✓	✓	✓	✓	✓	✓
BS switch on/off	✓	-	-	✓	-	-	✓	✓	✓	✓	✓	✓	✓	✓	-	✓	✓	-	✓	-	✓
Optimal solution	✓	-	✓	✓	✓	-	-	✓	✓	✓	✓	✓	✓	-	-	-	-	✓	✓	✓	✓
Heuristic solution	✓	✓	-	✓	✓	✓	✓	✓	✓	✓	✓	✓	✓	✓	✓	✓	✓	✓	-	✓	✓

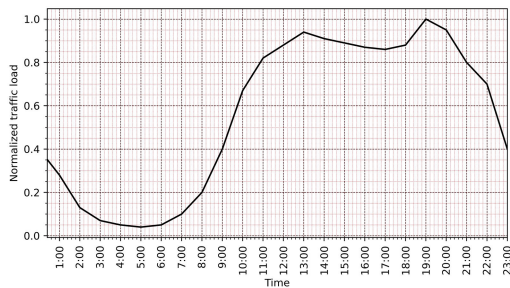


FIGURE 2. Average traffic load profile over one day.

where  $L(d_0)$  is the path loss in decibels (dB) at a reference distance of  $d_0$  meters between the transmitter and the receiver,  $\eta$  is the least square fits of the floating intercept and slope over the measured distances up to 200 meters,  $\sigma^2$  is the variance of the lognormal shadowing,  $\xi$  represents a normally distributed random variable with mean 0 and variance  $\sigma^2$ , and  $\lambda$  is the wavelength.

The received signal power  $P_{rx}^{su}$  for a given user equipment  $u$  UE at distance  $d$  from a given BS  $s$  can be calculated using the expression:

$$P_{rx}^{su} = P_{tx}^{su} + G_{tx} - L(d) + G_{rx} \quad (5)$$

where  $P_{tx}^{su}$  is the transmitted power from BS  $s$  to UE  $u$ , and  $G_{tx}$  and  $G_{rx}$  are the gains of the transmitter and receiver antennas, respectively. The antenna gain can be calculated as follows [44]:

$$G = 20 \log_{10} \left( \frac{\pi \cdot l}{\lambda} \right) \quad (6)$$

where  $l$  is the antenna length, either for the BS or the UE. While  $\lambda$  is the wavelength based on the used frequency. The transmission power  $P_{tx}^{su}$  from BS  $s$  to UE  $u$  must satisfy the power constraint.

$$\sum_{u \in U} P_{tx}^{su} \leq P_{max,s} \quad (7)$$

where  $P_{max,s}$  is the maximum RF output power of BS  $s$  at its maximum traffic load. The signal-to-interference-plus-noise ratio (SINR) for user  $u$  ( $u \in U$ ) from BS  $s$  ( $s \in S$ ) is given by

$$SINR_{su} = \frac{P_{su}^{rx} L(d_{su})}{I_s + P_n} \quad (8)$$

where  $I_s$  is the inter-cell interference and  $P_n$  is the additive white Gaussian noise power. The interference  $I_s$  caused by other BSs can be calculated as

$$I_s = \sum_{n \in S, n \neq s} P_{tx}^{nu} L(d_{nu}) \quad (9)$$

while  $P_n$  can be calculated using the expression

$$P_n = -174 + 10 \log(B) \quad (10)$$

where  $B$  is the bandwidth in Hertz (Hz).

According to Shannon's capacity formula we can determine the maximum achievable throughput (data rate)  $R_{su}$  for user  $u$  from BS  $s$  as follows:

$$R_{su} = B \cdot \log_2(1 + SINR_{su}) \quad (11)$$

### C. USER MOBILITY MODEL

In wireless networks, user mobility plays a crucial role in network performance and resource allocation. There are various methods to model the user mobility. For more details, a comprehensive survey on the different mobility models is presented in [41]. One way to model user mobility is through the use of the random walk model. The random walk model is a stochastic process that describes the movement of a particle or entity in a random or unpredictable manner. In the context of user mobility, this means that the user's movement is not deterministic and can be influenced by various factors such as location, time, and other environmental factors. In this mobility paradigm, users travel from their current place to a new one by randomly selecting a direction and speed. Both, the new speed and the new direction are picked from predefined ranges,  $[0, v_{max}]$  and  $[0, 2\pi]$ , where  $v_{max}$  represents the maximum walking speed. Figure 3 illustrates an example of user mobility based on the random walk scenario. In this work, we consider that users can only move inside the predefined area.

### D. USER GEOGRAPHICAL DISTRIBUTION

In this paper, we investigate user distributions categorized into two distinct distributions: uniform and non-uniform. The uniform distribution represents a scenario where the user equipment (UE) is uniformly distributed throughout the network, as illustrated in Fig. 4. Conversely, the non-uniform

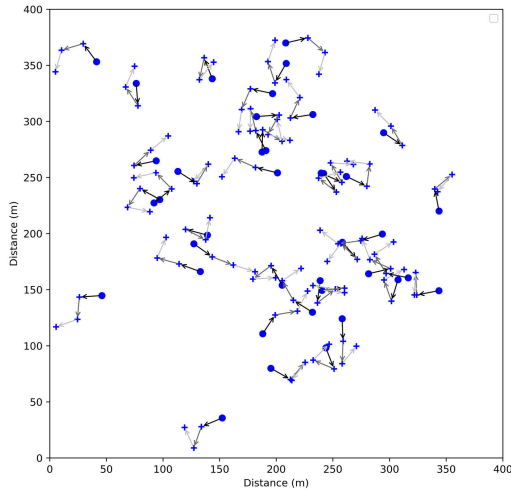


FIGURE 3. Example of random walk user mobility scenario for 40 users.

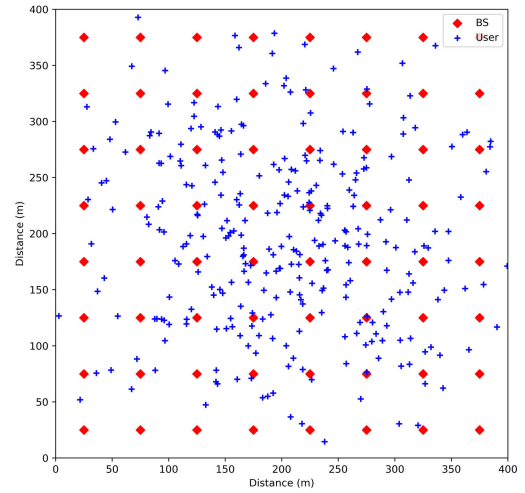


FIGURE 5. Nonuniform distribution for 400 users.

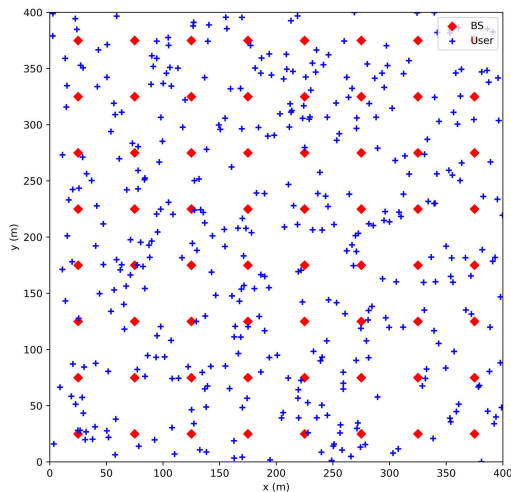


FIGURE 4. Uniform distribution for 400 users.

distribution represents scenarios where the UE is distributed non-uniformly in the network, as depicted in Fig. 5. Where in this scenario, the users are more crowded close to the center of the area. It can be done by generating random coordinates for the users based on a Gaussian distribution with a specified mean (the center of the area) and standard deviations of e.g. 85 meters. This distribution causes users to be more concentrated around the center of the area. Through this analysis, we aim to gain insights into the impact of these traffic models on network behavior.

**E. PROBLEM FORMULATION AND PROPOSED SOLUTIONS**

In this work we focus on the allocation of UEs and BSs, and energy consumption minimization. We refer to this problem as dual connectivity user and power allocation (DC- UPA) in 5G mmWave networks. Given a set of possible locations for BSs ( $S$ ), set of possible locations for users  $U$ , the objective of our problem is to minimize the power consumption by

reducing the number of active BSs and by ensuring that each user is to be assigned to two BSs whenever possible, while maintaining the QoS of the UEs. Optimization parameters are defined as follows:

- $k$ : a large number (i.e., 10000) (the higher the value of  $k$ , the larger the number of users with dual connectivity)
- $P_a$ : Power consumption per unit time for an active BS.
- $P_i$ : Power consumption per unit time for an inactive BS.
- $|U|$ : Number of users.
- $|S|$ : Number of BSs.
- $d_{max}$ : Maximum reach between an UE and a BS.
- $Th_{min}$ : Minimum throughput required for each user.
- $U_{max}$ : Maximum number of users allowed in each BS.
- $P_{max}$ : Maximum transmitted power of the BS.

Decision variables are defined as follows:

- $x_{us}$  is binary variable to describe the connectivity information of UEs and BSs. It indicates whether UE  $u$  is assigned to BS  $s$  as follows:

$$x_{us} = \begin{cases} 1 & \text{if UE } u \text{ is assigned to BS } s \\ 0 & \text{otherwise} \end{cases} \quad (12)$$

The association matrix between UEs and BSs is indicated by matrix  $X$  as follows:

$$X = \begin{bmatrix} x_{11} & \cdots & x_{1S} \\ \vdots & \ddots & \vdots \\ x_{U1} & \cdots & x_{US} \end{bmatrix}$$

- $z_u$  is a binary variable indicating that user  $u$  is assigned to two BSs or one BS, where:

$$z_u = \begin{cases} 1 & \text{if UE } u \text{ is allocated to one BS} \\ 0 & \text{if UE } u \text{ is allocated to two BSs} \end{cases} \quad (13)$$

- $y_s$  is a binary variable indicating that the BS  $s$  is in active or sleep mode:

$$y_s = \begin{cases} 1 & \text{if BS } s \text{ is active} \\ 0 & \text{if BS } s \text{ is inactive} \end{cases} \quad (14)$$

where

$$y_s = \lceil \frac{\sum_{u \in U} x_{us}}{U_{max}} \rceil, \quad \forall s \in S \quad (15)$$

That means,  $y_s = 1$  if at least one user  $u$  is connected to it, and  $y_s = 0$  if no user  $u$  is connected to that BS  $s$ .

### Objective function 1.

$$\text{minimize} \left\{ \sum_{s \in S} (y_s \cdot P_a + (1 - y_s) \cdot P_i) + k \cdot \sum_{u \in U} z_u \right\} \quad (16)$$

Subject to:

- 1) User allocation constraint: Each user can be assigned to either two or a single BSs at a time represented as follows:

$$\sum_{s \in S} x_{us} = 2 - z_u, \quad \forall u \in U \quad (17)$$

- 2) Active BS constraint: Each BS must be active if at least one user is assigned to it:

$$y_s \geq x_{us}, \quad \forall u \in U, s \in S \quad (18)$$

- 3) Switching off BS constraint: If there is no single user assigned to a BS then it is switched off:

$$\sum_{s \in S} x_{us} \geq y_s, \quad \forall s \in S \quad (19)$$

- 4) Upper bound on the number of allocated users: The maximum number of users allocated to a BS must not exceed  $U_{max}$  the maximum number of connections per BS:

$$\sum_{s \in S} x_{us} \leq U_{max}, \quad \forall s \in S \quad (20)$$

- 5) Transmitted power constraint: The total transmission power may not exceed the maximum value  $P_{max}$ :

$$\sum_{u \in U} x_{us} \cdot P_{tx}^{su} \leq P_{max}, \quad \forall s \in S \quad (21)$$

- 6) QoS constraint: The data rate  $R_{us}$  allocated to each user must be at least equal to the minimum threshold  $Th_{min}$ :

$$R_{us} \geq Th_{min} \cdot x_{us}, \quad \forall u \in U, s \in S \quad (22)$$

- 7) Transmission distance constraint: The distance  $d_{us}$  between user  $u$  and BS  $s$  must be less or equal the maximum allowed distance  $d_{max}$ :

$$x_{us} \cdot d_{us} \leq d_{max}, \quad \forall u \in U, s \in S \quad (23)$$

- 8) Binary variables constraint:

$$x_{us}, y_s, z_u \in \{0, 1\} \quad \forall u \in U, s \in S \quad (24)$$

In the case of a single connectivity scenario, where each user can be connected to one BS only, the ILP is reformulated as follows:

### Objective function 2.

$$\text{minimize} \left\{ \sum_{s \in S} (y_s \cdot P_a + (1 - y_s) \cdot P_i) \right\} \quad (25)$$

Subject to:

- 1) User allocation constraint: Each user can be assigned to only one BSs at a time, and given as follows:

$$\sum_{s \in S} x_{us} = 1, \quad \forall u \in U \quad (26)$$

- 2) Constraints defined by Eqs. 18-24.

In order to maximize the total throughput of the system, the ILP is modified as follows:

### Objective function 3.

$$\text{maximize} \left\{ \sum_{u \in U} \sum_{s \in S} x_{us} \cdot R_{us} - k \cdot \sum_{u \in U} z_u \right\} \quad (27)$$

Subject to: constraints given by Eqs. 17-24.

*Proposition 1: The optimization problem formulated in Eq. 16 is an NP-hard one.*

*Proof:* The problem presented in Eq. 16 contains the sub-problem of assigning each user to two BSs simultaneously, which can be formulated as a variant of the set cover problem, a well-known NP-hard problem [43]. To see this, let us consider the following reduction:

- 1) Define a set  $S_u$  for each user  $u$ , where  $S_u$  contains all the BSs to which  $u$  can be assigned.
- 2) Define a universe  $U$  as the union of all sets  $S_u$ .
- 3) Define a collection  $C$  of subsets of  $U$ , where each subset  $c$  corresponds to a pair of BSs that can be assigned to a user simultaneously. Specifically, for each user  $u$ , we can define a collection (a superset) of subsets of  $S_u$ , each containing two BSs to which  $u$  can be assigned simultaneously. The union of all such subsets for all users  $u$  gives us the  $C$ .
- 4) The problem of assigning each user to two BSs simultaneously can now be formulated as finding the minimum number of subsets in  $C$  that cover the universe  $U$ , where each subset corresponds to a pair of BSs that can be assigned to a user simultaneously.

This reduction shows that the problem is at least as hard as the set cover problem, known as NP-hard. Therefore, the problem of assigning each user to two BSs simultaneously is also NP-hard. As the sub-task of the problem is NP-hard, the presented problem is an NP-hard one, as well.

### F. HEURISTIC APPROACH FOR DC-UPA PROBLEM

The ILP provides the optimal solution for the proposed problem. However, for large-size problems, the ILP becomes time-consuming and computationally ineffective. On the

other hand, heuristic methods require a lower running time to find sub-optimal solutions with acceptable quality. However, since they do not guarantee the optimal solution, we can compare the results obtained by the heuristic approaches to the optimal solution obtained from the ILP model to determine the quality of the heuristic solutions.

Figure 6 shows the example comparison of the ILP, SA, and DA running time for different number of users under the uniform users distribution. The results indicate that both SA and DA algorithms outperform ILP in terms of computational efficiency, as they require less time to find sub-optimal solutions.

For that due to the complexity of the DC-UPA problem stated in Eq. 16, obtaining the optimal solution using the ILP is valid only for deployment scenarios with a limited number of BSs and users (as shown in Fig. 6 the running time of the ILP grows particularly for the number of users more than 150). As the number of users in real scenarios in the real-world deployments is typically even greater than 150, we have developed two computationally efficient heuristic algorithms specifically tailored to address the challenges of DC-UPA for large-scale problems: The Simulated Annealing (SA) algorithm and Distance-Aware (DA) greedy algorithm. While the ILP can solve the problem simultaneously, SA and DA solve it as a sequence (decompose) of two sub-problems (i.e., user allocation problem followed by the power allocations problem). As shown later in our paper, these algorithms offer effective solutions to tackle the complexity of the problem.

### 1) SIMULATED ANNEALING (SA) ALGORITHM

SA is a general meta-heuristic algorithm, and allows for finding high-quality solutions to the DC-UPA problem by exploring the solution space while avoiding getting stuck in local optima. The pseudo code for the proposed SA algorithm for solving DC-UPA is illustrated in Algorithm 1. The main steps of the proposed SA approach are summarized as follows:

- Step 1: The SA takes as input the following parameters: cooling rate  $\alpha$ , initial temperature  $T_0$ , final temperature  $T_f$ , maximum distance  $d_{max}$ ,  $P_a$ ,  $P_i$ , distance matrix  $D$ ,  $|U|$ ,  $|S|$ , throughput matrix  $Th$ ,  $P_{max}$ , and  $U_{max}$ . The algorithm returns the best solution  $S_{best}$ , the best power consumption  $P_{best}$ , and the set of active BSs  $A$ .
- Step 2: Create an initial solution matrix  $S_0$  of the size of the number of users x number of BSs with all elements initially set to 0. For each user, find valid BSs that meet the constraints (distance, throughput) and select the first two BSs from the shuffled list of valid BSs, if there are at least two valid BSs. If there is only one valid BS, select that BS. Set the corresponding elements of the solution matrix to 1.
- Step 3: Set the current solution  $S_{current}$  to  $S_0$ , and initialize the best solution  $S_{best}$  to  $S_{current}$ .

### Algorithm 1 Simulated Annealing Algorithm (SA) for DC-UPA Problem

**Require:** Initial solution matrix  $S_0$ ; cooling rate  $\alpha$ ; initial temperature  $T_0$ ; final temperature  $T_f$ ;  $d_{max}$ ;  $P_a$ ;  $P_i$ ; distance matrix  $D$ ; Coordinates matrix  $C$ ;  $|U|$ ;  $|S|$ ; throughput matrix  $Th$ ;  $P_{max}$ ;  $U_{max}$ ;  $Th_{min}$ .

**Ensure:** The best solution  $S_{best}$ , the best power consumption  $P_{best}$ , Number of active BSs  $A$ .

```

1: initialize  $S_0$  of size num_users x num_BSs with all
   elements set to 0
2: for each user  $u$  do
3:   Find valid_BSs for user  $u$  such that
   distance_matrix[ $u, s$ ]  $\leq d_{max}$ , and  $Th[us] \geq Th_{min}$ 
4:   shuffle valid_BSs
5:   if length(valid_BSs)  $\geq 2$  then
6:     Select the first two BSs from valid_BSs as
     selected_BSs
7:   else
8:     Select the first BS from valid_BSs as
     selected_BSs
9:   for each BS  $s$  in selected_BSs do
10:    Set solution[ $u, s$ ] to 1
11:  $S_{current} \leftarrow S_0$ 
12:  $S_{best} \leftarrow S_{current}$ 
13:  $P_{current} \leftarrow$  Power consumption of  $S_{current}$ 
14:  $P_{best} \leftarrow P_{current}$ 
15:  $T \leftarrow T_0$ 
16:  $A \leftarrow$  [number of active cells in  $S_{best}$ ]
17:  $P \leftarrow [P_{best}]$ 
18: while  $T > T_f$  do
19:   create a copy of  $S_0$ 
20:   select a random user  $u$ 
21:   find valid_BSs for user  $u$  such that distance_matrix[ $u,$ 
    $c$ ]  $\leq d_{max}$ ,  $Th[us] \geq Th_{min}$ , number of users  $\leq U_{max}$ ,
   transmitted power  $\leq P_{max}$  and new_solution[ $u, s$ ] == 0
22:   if valid_BSs is empty then
23:     continue
24:   select a random BS  $s1$  from valid_BSs
25:   find assigned_BSs for user  $u$  where new_solution[ $u,$ 
    $s$ ] == 1
26:   select a random BS  $s2$  from assigned_BSs
27:   set new_solution[ $u, s1$ ] to 1
28:   set new_solution[ $u, s2$ ] to 1
29:    $P_{new} \leftarrow$  energy consumption of  $S_{new}$ 
30:    $\Delta P \leftarrow P_{new} - P_{current}$ 
31:    $p \leftarrow$  random number between 0 and 1
32:   if  $\Delta P < 0$  or  $p < e^{-\Delta P/T}$  then
33:      $S_{current} \leftarrow S_{new}$ 
34:      $P_{current} \leftarrow P_{new}$ 
35:     if  $P_{current} < P_{best}$  then
36:        $S_{best} \leftarrow S_{current}$ 
37:        $P_{best} \leftarrow P_{current}$ 
38:        $A.append$ (number of active cells in  $S_{best}$ )
39:        $P.append$ ( $P_{best}$ )
40:    $T \leftarrow T * \alpha$ 
41: return  $S_{best}$ ,  $P_{best}$ ,  $A$ ,  $P$ 

```



- Step 4: Calculate the power consumption of the current solution  $P_{\text{current}}$  and set the best solution  $P_{\text{best}}$  to  $P_{\text{current}}$ .
- Step 5: Initialize the temperature  $T$  to  $T_0$ , and create lists to store the number of active BSs  $A$  and power consumption  $P$ .
- Step 6: While the temperature  $T$  is higher than the final temperature  $T_f$ , perform the following steps iteratively:
  - 1) Create a new solution by copying the current solution and randomly selecting a user.
  - 2) Find valid BSs for the selected user based on the constraints (distance, throughput, maximum users, and transmitted power).
  - 3) If there are no valid BSs, go to (1).
  - 4) Randomly select two BSs from the valid BSs or at least one BS (based on the column of the set of BSs that meet the constraints), and update the new solution accordingly.
  - 5) Calculate the energy consumption of the new solution  $P_{\text{new}}$  and the change in energy consumption  $\Delta P$ .
  - 6) Generate a random number  $p$  between 0 and 1.
  - 7) If  $\Delta P < 0$  (better solution) or  $p < e^{-\Delta P/T}$  (acceptance probability), update the current solution and its power consumption accordingly. If the current solution's power consumption is less than the best solution's, update the best solution, its power consumption, and append the number of active BSs and power consumption to the respective lists.
  - 8) If the new solution is not accepted, reject it.
  - 9) Update the temperature by multiplying it with the cooling rate  $\alpha$ .
- Step 7: Return the best solution  $S_{\text{best}}$ , the best power consumption  $P_{\text{best}}$ , and the lists of active BSs  $A$  and power consumption  $P$ .

## 2) DISTANCE AWARE (DA) GREEDY ALGORITHM

The DA algorithm is a simplified method for solving the DC-UPA problem, where users are assigned to BSs by assigning each user to the two closest BSs considering the distance constraints and the BSs capacities. Then, the total power consumption of the network is calculated regarding the active and inactive BSs. The pseudo-code for the proposed DA algorithm is presented by Algorithm 2. The step-by-step description is as follows:

- Step 1: Assign users to the two closest BSs. Initially, users are assigned to their two closest BSs that are within the maximum distance  $d_{\text{max}}$ .
- Step 2: Initialize array  $A$  of length  $|S|$  (number of BSs) with all elements set to (*False*) (inactive). Each element of the array represents whether a BS is active or inactive.
- Step 3: Iterate through each user  $u$  from 1 to  $|U|$  (number of users), and perform the following steps:
  - 1) Find the two closest BSs to the user  $u$  that are within the maximum distance  $d_{\text{max}}$ .

### Algorithm 2 Distance Aware (DA) Greedy Algorithm for DC-UPA Problem

**Require:** Coordinates matrix  $C$ ; distance matrix  $D$ ;  $d_{\text{max}}$ ;  $U_{\text{max}}$ ;  $p_a$ ;  $p_i$

**Ensure:** Power consumption  $P$ ; number of active BSs  $n_a$ .

- 1: Assign users to closest two BS.
- 2:  $A \leftarrow$  Boolean array of length  $|S|$  initialized to all **False**
- 3: **for**  $u = 1$  to  $|U|$  **do**
- 4: Find the two closest BSs to user  $u$  that are within  $d_{\text{max}}$
- 5:  $C_u \leftarrow$  Indices of the two closest BSs in ascending order of distance
- 6: **for**  $i = 1$  to 2 **do**
- 7: **if**  $D_{u,C_u(i)} \leq d_{\text{max}}$  and  $u_{C_u(i)} < U_{\text{max}}$  and  $A_{C_u(i)} = \mathbf{False}$  **then**
- 8:  $A_{C_u(i)} \leftarrow \mathbf{True}$
- 9:  $u_{C_u(i)} \leftarrow u_{C_u(i)} + 1$
- 10: **break**
- 11: Count active and inactive BSs:
- 12:  $n_a \leftarrow$  Number of active BSs,  $n_i \leftarrow |S| - n_a$
- 13: Switch off the BSs that are not assigned to any user.
- 14: **for**  $i = 1$  to  $n_c$  **do**
- 15: **if**  $A_i = \mathbf{False}$  **then**
- 16:  $A_i \leftarrow \mathbf{True}$
- 17: Calculate power consumption
- 18:  $P \leftarrow n_a \cdot p_a + n_i \cdot p_i$
- 19: **return**  $P, n_a$

- 2) Get the indices of these two closest BSs in ascending order of distance and store them in  $C_u$ .
- 3) For each of the two closest BSs, check the following conditions:
  - a) The distance between the user and the BS should be less than or equal to  $d_{\text{max}}$ .
  - b) The BS should have available capacity (the number of users in the BS should be less than  $U_{\text{max}}$ ).
  - c) The BS should be inactive ( $A_{C_u(i)}$  should be *False*).
  - d) If all the above conditions are satisfied, mark the BS as active by setting  $A_{C_u(i)}$  to (*True*), increment the user count in the BS by 1, and break out of the inner loop.

- Step 4: Count the active and inactive BSs in the network. Let  $n_a$  be the number of active BSs and  $n_i$  be the number of inactive BSs, where  $n_i = |S| - n_a$ .
- Step 5: Switch off the BSs that are not assigned to any user by setting the corresponding elements in the array  $A$  to (*True*).
- Step 6: Calculate the total power consumption  $P$  as the sum of the power consumption of all active and inactive BSs, i.e.,  $P = n_a \cdot p_a + n_i \cdot p_i$ .
- Step 7: Return the total power consumption  $P$  as the output of the algorithm.

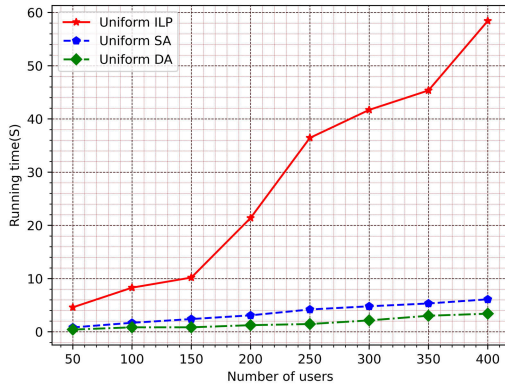


FIGURE 6. Runtime comparison for the ILP, SA, and DA for different number of users in the case of uniform distribution.

### 3) COMPLEXITY ANALYSIS

The time complexity of the proposed heuristic algorithms can be expressed as follows. For the SA, it has a time complexity of  $O(|U| \cdot |S|^3 \cdot \log(T_0/T_f) / \log(\alpha))$ , while the time complexity of the DA is  $O(|U| \cdot |S|^2)$ . Polynomial complexity of SA and DA approaches, in turn, confirms their usability in common real-world deployment scenarios involving several hundreds of users.

## IV. SIMULATION RESULTS AND DISCUSSION

### A. PARAMETER SETUP

In this section, we analyze the performance of various proposed methods, where the performance of the ILP, SA, and DA approaches is evaluated through simulations in a two-dimensional area, denoted as  $A$ , with the size of 400m x 400m. To obtain the optimal solutions, we utilize the commercially available CPLEX solver, which was run on a machine equipped with an Intel(R) Core(TM) i5-1035G1 CPU operating at 1.00GHz and 8GB RAM. The SA and DA simulations were implemented using Python programming language.

Several parameters were considered for the simulation, as summarized in Table. 2.

### B. RESULTS AND DISCUSSION

Initially, we conducted a comparison of the optimal power consumption of the network under single and dual connectivity in both uniform and nonuniform distribution scenarios, as illustrated in Fig. 7. The figure demonstrates that when considering uniform distributions with single connectivity, the power consumption required for 50, 200, and 400 users is 472.8, 587.19, and 618.4 W, respectively. On the other hand, for uniform distributions of users locations with dual connectivity and the same number of users, the power consumption is 618.4, 868, and 920 W, respectively. This means that, on average, dual connectivity requires 30% more power than single connectivity. When considering a nonuniform distribution with single connectivity, the power consumption values are (503.99, 680.97, 805.59)

TABLE 2. Simulation parameters [38], [44].

Parameter	Value
Area size ( $A$ )	400m x400m
BS radius ( $d_{max}$ )	50, 75, 100 m
Number of users $ U $	50, 100, ...,400
Number of BSs ( $ S $ )	64
Frequency	28 GHz
Bandwidth ( $B$ )	1200 MHz
$d_0$	1 m
$L(d_0)$	61.4
$\eta$	2.1
$P_{max}$	30 dbm
$\xi$	5.8
$v_{max}$	1.3 m/s
$\lambda$	10.7 mm
$l(tx)$	0.1 m
$l(rx)$	0.01 m
$P_a$	14.7 W
$P_i$	4.3 W
$U_{max}$	20
$Th_{min}$	19.3 Mbps
$T_0$	100
$T_f$	0.01
$\alpha$	0.99

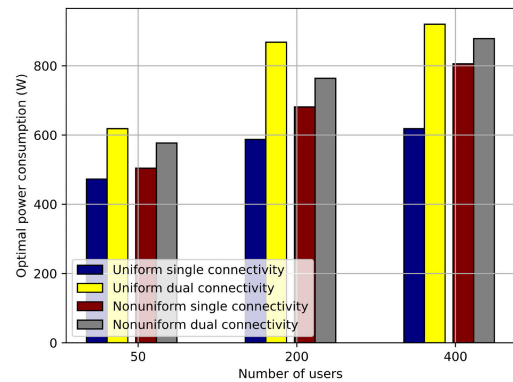
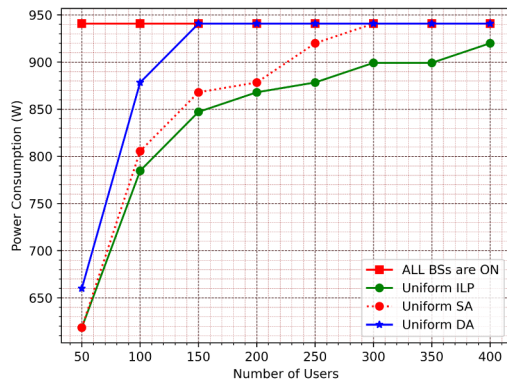


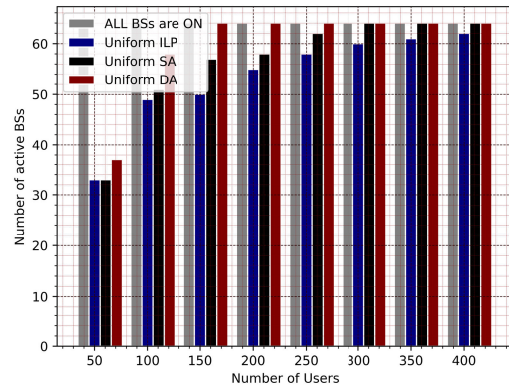
FIGURE 7. The optimal power consumption of single connectivity vs. dual connectivity scenarios as a function of the number of users (uniform and nonuniform distributions).

W, respectively. On the other hand, for dual connectivity, the power consumption values are higher at 576.79, 763.99, and 878.39 W. This indicates that dual connectivity requires approximately 10% more power than single connectivity.

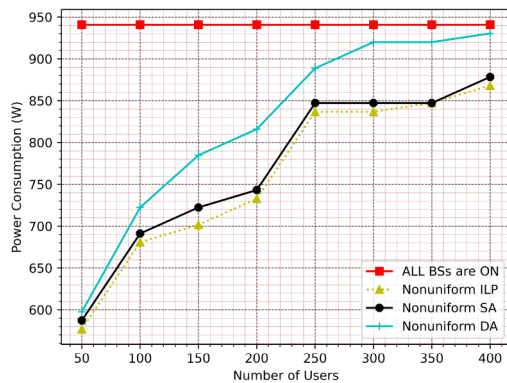
Although dual connectivity leads to increased power consumption compared to single connectivity in uniform or nonuniform scenarios within 5G networks, it is crucial to prioritize resilience for ultra-reliable low-latency communication (URLLC) services. This resilience can be enhanced by incorporating redundancy, which means connecting each user to two or more BSs instead of just one. Additionally, the channel becomes less reliable at higher frequencies (such as millimeter-wave and near-terahertz), making non-line-of-sight (NLOS) conditions, fading, and reaching even more critical factors to consider. This study primarily emphasizes optimizing the power consumption and user allocation (dual connectivity).



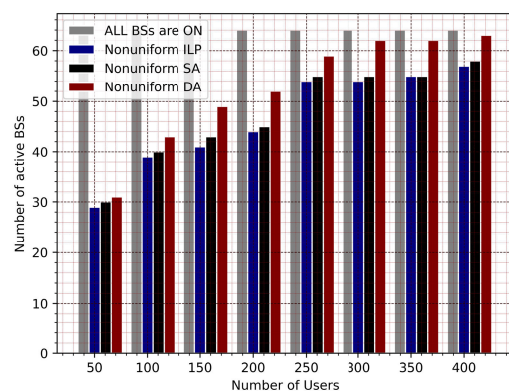
(a) Network power consumption vs. number of users (uniform distribution)



(a) The number of active BSs vs. number of users (uniform distribution)



(b) Network power consumption vs. number of users (nonuniform distribution)



(b) The number of active BSs vs. number of users (nonuniform distribution)

**FIGURE 8.** Network power consumption as a function of the number of users using the proposed solutions.

Figure 8 illustrates a comparison of network power consumption for scenarios of various number of users (50, 100, ..., 400), considering different proposed solutions (ILP, SA, and DA). The graph presented in Fig. 8(a) shows the power consumption when users are uniformly distributed in the area. It is evident that the ILP (providing the optimal solution) yields the lowest power consumption, outperforming the scenario where all cells are switched on. SA demonstrates a performance close to the ILP, delivering superior results compared to DA. In the case of DA, higher power consumption occurs, as it attempts to connect each user to the two closest cells, necessitating the activation of additional BSs. For instance, in the case of the number of users equal 150, the power consumption provided by the ILP equals to 847 W, while SA implies in 868.0 W, finally, 940.8 W for DA.

Figure 9(a) compares the number of active BSs as a function of the number of users in the case of the optimal deployment, where the number of active BSs has the same trend as Fig. 8(a) in terms of the performance of the proposed solutions. Additionally, Fig. 8(b) shows the power consumption when users are nonuniformly distributed within the area, where there are more users located closer to the

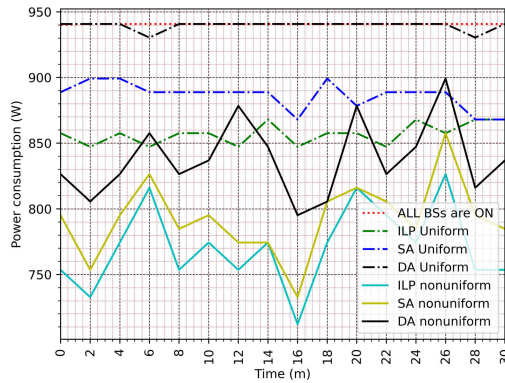
**FIGURE 9.** The number of active BSs as a function of the number of users using the proposed solutions.

center and fewer users near the borders of the area. It is evident from the graph that a significant reduction in power consumption occurs compared to the uniform distribution. This reduction is attributed to the lower number of users outside the center area, enabling deactivation of more BSs in those regions, as it is illustrated in Fig. 9(a), compared to Fig. 9(b).

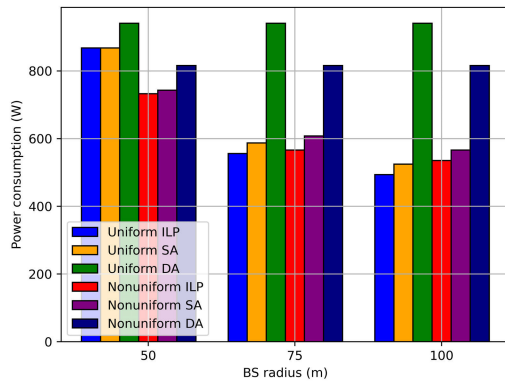
Notably, the performance of DA is improved for this nonuniform distribution scenario, compared to the uniform distribution case. In the central area with higher user density, the proximity of users to BSs prompts the ILP and SA approaches to connect users to the closest cells, resembling the behavior of DA. This leads to DA performing better in terms of power consumption in such cases.

Figure 10 illustrates the dynamic changes in power consumption over time resulting from the movement of users according to the random walk mobility model. The experiment involves 200 users and a BS with a radius of 50 m. The graph demonstrates that the power consumption in the uniform distribution case is significantly higher than in the nonuniform distribution scenario. Nevertheless, both scenarios exhibit fluctuations due to the dynamic changes in the network configuration, with the nonuniform scenario

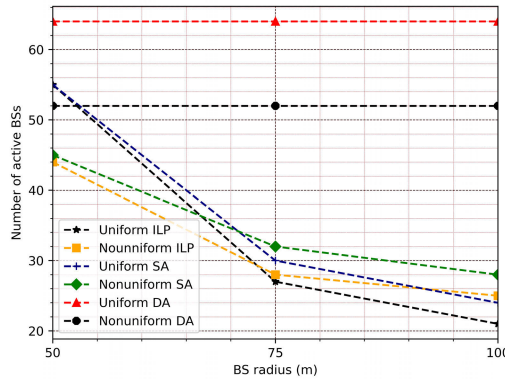




**FIGURE 10.** The network power consumption for the case of 200 users and BS radius of 50 m over time for uniform and nonuniform distributions of users locations.



(a) The network power consumption and the number of active BSs as a function of the BS radius.

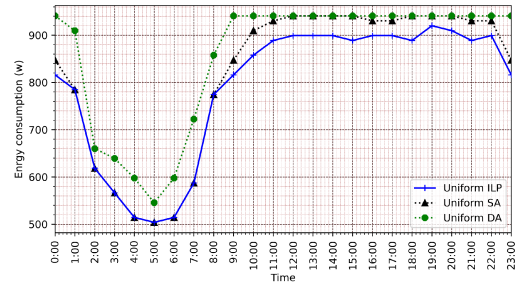


(b) The number of active BSs vs. number of users

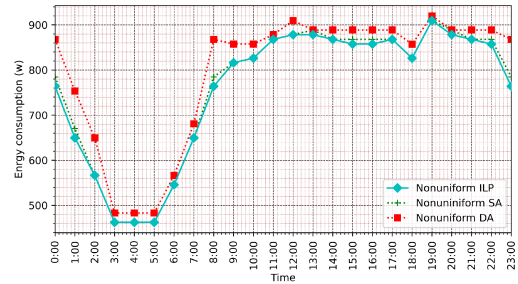
**FIGURE 11.** The impact of the BS radius on the power consumption and the number of active BSs using the proposed solutions for the case of 200 users.

showing more pronounced variations for a single simulation run.

The average power consumption values for the uniform distribution case obtained through the ILP, SA, and DA algorithms are 856.94 W, 886.19 W, and 939.49 W, respectively. In contrast, the average power consumption values for the nonuniform distribution case are 771.14 W, 792.59 W,



(a) Network power consumption behavior during 24 hours of operation (uniform distribution)



(b) Network power consumption behavior during 24 hours of operation (nonuniform distribution)

**FIGURE 12.** The network power consumption profile over a day of operation.

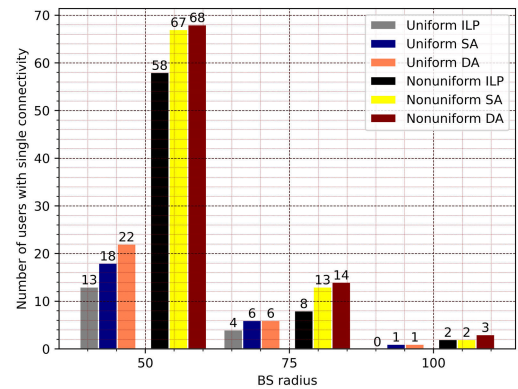


**FIGURE 13.** The number of users with single connectivity using the proposed solutions in the case of 400 users vs. BS radius.

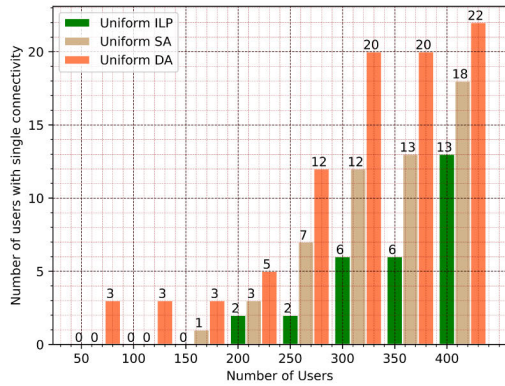
and 838.09 W, generated by the ILP, SA, and DA methods, respectively.

Figure 11(a) illustrates the values of power consumption as a function of the BS radius, considering both uniform and nonuniform distributions. Fig. 11(b) presents the variations in the number of active BSs with respect to the BS radius.

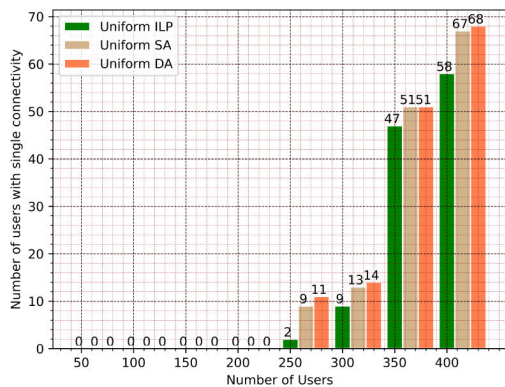
We take into account three different values for the BS radius: 50 m, 75 m, and 100 m. Notably, as the radius increases, both the power consumption and the number of active BSs decreases, regardless of whether the distribution is uniform or nonuniform.

It is evident that there is no change in the performance of the DA algorithm, as it always connects the user to the two closest BSs, regardless of the radius. However, when





(a) Network power consumption behavior during 24 hours of operation (uniform distribution)



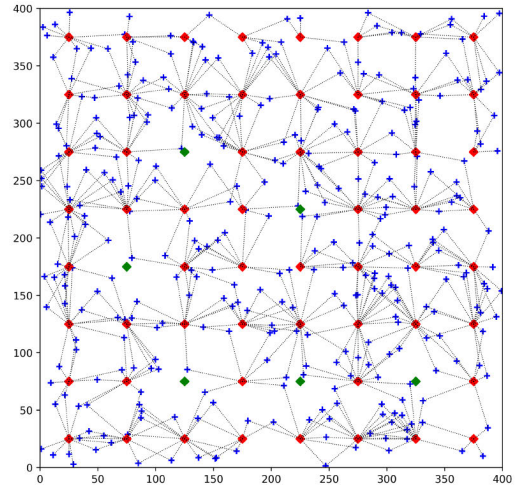
(b) Network power consumption behavior during 24 hours of operation (nonuniform distribution)

**FIGURE 14.** The number of single connected users as a function of the total number of users with the BS radius equals to 50 m.

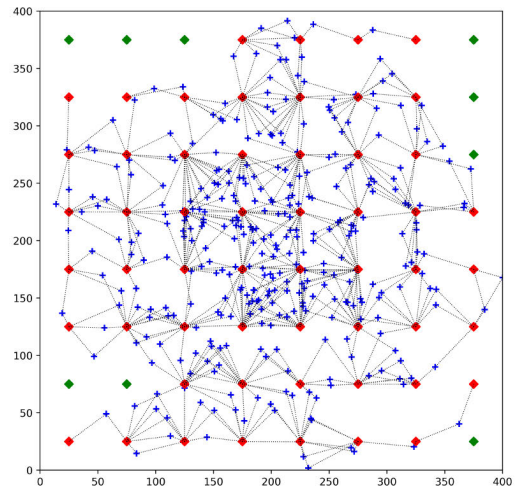
the BS radius becomes larger, both ILP and SA algorithms consistently outperform DA. This finding suggests that while DA is particularly useful for dense networks with shorter radii, ILP and SA exhibit superior performance in the case of networks with larger radii.

Figure 12 illustrates the dynamic changes in the network power consumption profile throughout the day, showing the results obtained for the proposed solutions (ILP, SA, DA). In particular, Fig. 12(a) presents characteristics for the case of a uniform distribution, while Fig. 12(b) refers to the scenario with a nonuniform distribution. It is noteworthy that both SA and ILP exhibit comparable performance in both distribution scenarios, closely aligned in terms of power consumption. Conversely, the DA solution demonstrates inferior performance in the case of a uniform distribution.

However, as locations of users become denser and closer to the BSs, the DA solution proves to be more effective for the nonuniform distribution scenario, where, in the case of a uniform distribution, the daily average power consumption is found to be 789.55 W, 814.7 W, and 857.6 W for the ILP, SA, and DA, respectively with the optimality gap of 8.62% for the DA. Additionally, for the nonuniform distribution, the



(a) Optimal users assignment (uniform distribution)



(b) Optimal users assignment (nonuniform distribution)

**FIGURE 15.** Optimal UEs-BSs assignment in the case of 350 users.

daily average power consumption is measured at 756.17 W, 761.82 W, and 795.62 W for the ILP, SA, and DA, respectively, with the optimality gap of 5.2% for the DA.

In other words, the obtained power consumption reduction over the day in the case of the uniform distribution is up to 16.1%, and in the case of the nonuniform distribution is up to 20%. Furthermore, it is noteworthy that the power consumption over the day is influenced by the traffic profile, which is illustrated in Fig. 2.

Figure 13 illustrates the relationship between the number of users with single connectivity and the radius of the BS in the case of 400 users in the area. It is evident from Fig. 13 that the number of single-connected users decreases as the BS radius increases.

Additionally, the figure highlights that in the case of a nonuniform distribution, the number of single-connected users is higher than for a uniform distribution for all three BS radius lengths (50 m, 75 m, and 100 m).

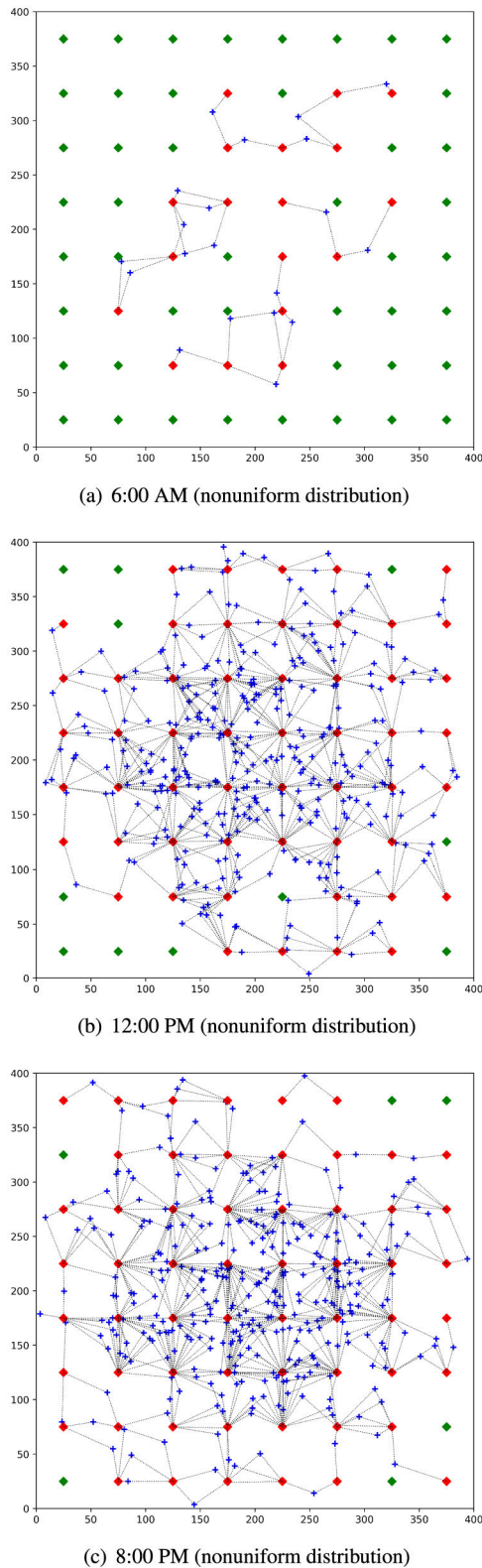


**FIGURE 16.** Example users-BSs assignment at 6:00 AM, 12:00 PM, and 8:00 PM.

However, the disparity becomes more pronounced when the BS radius is 50 m. This can be attributed to the higher user density in the central area of the region in the nonuniform

distribution scenario. Consequently, most of the BSs in the central area become overloaded, resulting in the inability to simultaneously connect each user to two BSs, where the single connectivity ratio may reach up to 17%.

Additionally, Figs. 14(a) and 14(b) depict the relationship between the number of single-connected users as a function of the number of users in both uniform and nonuniform distributions, respectively.

The analysis shows that for high-density user scenarios (more than 250 users), the nonuniform distribution exhibits a significantly higher number of single-connected users. This phenomenon can be attributed to the overload experienced by BSs located in the center of the area, resulting in inadequate coverage for users located close to the center. In other words, the network cannot provide dual connectivity for all users closer to the center. Specifically, when considering 400 users, the average percentage of users with single connectivity is determined as follows: ILP (14%), SA (16.75%), and DA (17%) based on the applied optimization techniques.

In contrast, the uniform distribution yields a considerably lower number of users with single connectivity due to the effective load balancing among all BSs in the area. In this case, when analyzing the scenario with 400 users, the average percentage of single-connected users is observed to be: 3.25%, 4.5%, and 5.5% as obtained through the ILP, SA, and DA methods, respectively. These results highlight the ability of the uniform distribution to distribute the user load evenly across the network, thereby enhancing the overall connectivity experience.

Figure 15 presents the optimal association between users and BSs in a scenario involving 350 users, where, in Fig. 15(a) the users are uniformly distributed across the area. The blue pluses represent the users, the red lozenges symbolize the active BSs, and the green lozenges depict the inactive BSs, while, Fig. 15(b), shows the optimal associations for the same number of 350 users, but this time considering a nonuniform distribution scenarios.

Figure 16 illustrates the dynamic association between users and BSs throughout a day in the case of nonuniform users distribution, highlighting three key time points: at 6:00 AM, in Fig. 16(a), 12:00 PM, in Fig. 16(b), and 20:00 PM. in Fig. 16(c). The BSs are selectively deactivated based on the fluctuating traffic load. Notably, during peak periods, such as 12:00 PM and 8:00 PM, there is a higher number of active BSs due to the increased traffic demand volume in these “peak hours” set compared to the morning period.

**V. CONCLUSION**

Determining a power-efficient network deployment that guarantees continuous coverage for the end user is an essential challenge for 5G and beyond wireless networks. In this paper, we proposed a joint dual connectivity and power allocation strategy to address that challenge. We mathematically formulated the Dual Connectivity User and Power Allocation (DC-UPA) problem as an ILP to obtain the optimal solution. Considering the complexity of the DC-UPA

problem and the scalability concerns associated with the ILP, we have also developed two heuristic algorithms: simulated annealing (SA) and distance-aware (DA). We run extensive simulations to demonstrate the viability of the proposed solution in a two-dimensional area with two different geographic user distributions (uniform and nonuniform). The obtained results show that, with the proposed solutions, the power consumption in 5G mmWave networks is significantly reduced in the two studied user distributions while at the same time guaranteeing continuous coverage for the end users thanks to the dual connectivity. We anticipate that our solutions can pave the way for improved network performance, enhanced user experience, and reduced energy consumption in future wireless networks.

In our future work, we will focus on integrating the energy harvesting techniques into network deployment strategies. Using renewable energy sources and incorporating green communication protocols can further enhance power efficiency and reduce the environmental impact of wireless networks. Moreover, we also plan to extend our research towards utilization of MIMO technology instead of involving only single antennas to further improve the system performance.

## REFERENCES

- [1] M. H. Alsharif, A. H. Kelechi, M. A. Albreem, S. A. Chaudhry, M. S. Zia, and S. Kim, "Sixth generation (6G) wireless networks: Vision, research activities, challenges and potential solutions," *Symmetry*, vol. 12, no. 4, p. 676, Apr. 2020, doi: [10.3390/sym12040676](https://doi.org/10.3390/sym12040676).
- [2] F. Tariq, M. R. A. Khandaker, K.-K. Wong, M. A. Imran, M. Bennis, and M. Debbah, "Speculative study on 6G," *IEEE Wireless Commun.*, vol. 27, no. 4, pp. 118–125, Aug. 2020, doi: [10.1109/MWC.001.1900488](https://doi.org/10.1109/MWC.001.1900488).
- [3] M. Agiwal, A. Roy, and N. Saxena, "Next generation 5G wireless networks: A comprehensive survey," *IEEE Commun. Surveys Tuts.*, vol. 18, no. 3, pp. 1617–1655, 3rd Quart., 2016, doi: [10.1109/comst.2016.2532458](https://doi.org/10.1109/comst.2016.2532458).
- [4] M. Giordani, M. Polese, M. Mezzavilla, S. Rangan, and M. Zorzi, "Toward 6G networks: Use cases and technologies," *IEEE Commun. Mag.*, vol. 58, no. 3, pp. 55–61, Mar. 2020, doi: [10.1109/mcom.001.1900411](https://doi.org/10.1109/mcom.001.1900411).
- [5] *6G Architecture Landscape—European Perspective. White Paper*. Accessed: May 15, 2023. [Online]. Available: <https://5g-ppp.eu/6g-architecture-landscape-europeanperspective-white-paper>
- [6] T. Sizer, D. Samardzija, H. Viswanathan, S. T. Le, S. Bidkar, P. Dom, E. Harstead, and T. Pfeiffer, "Integrated solutions for deployment of 6G mobile networks," *J. Lightw. Technol.*, vol. 40, no. 2, pp. 346–357, Jan. 2022, doi: [10.1109/jlt.2021.3110436](https://doi.org/10.1109/jlt.2021.3110436).
- [7] M. Xiao, S. Mumtaz, Y. Huang, L. Dai, Y. Li, M. Matthaiou, G. K. Karagiannidis, E. Björnson, K. Yang, C.-L. I, and A. Ghosh, "Millimeter wave communications for future mobile networks," *IEEE J. Sel. Areas Commun.*, vol. 35, no. 9, pp. 1909–1935, Sep. 2017, doi: [10.1109/jsac.2017.2719924](https://doi.org/10.1109/jsac.2017.2719924).
- [8] L. Zhu, Z. Xiao, X.-G. Xia, and D. O. Wu, "Millimeter-wave communications with non-orthogonal multiple access for B5G/6G," *IEEE Access*, vol. 7, pp. 116123–116132, 2019, doi: [10.1109/access.2019.2935169](https://doi.org/10.1109/access.2019.2935169).
- [9] S. Tripathi, N. V. Sabu, A. K. Gupta, and H. S. Dhillon, "Millimeter-wave and terahertz spectrum for 6G wireless," in *6G Mobile Wireless Networks*. Cham, Switzerland: Springer, 2021, pp. 83–121.
- [10] B. T. Tinh, L. D. Nguyen, H. H. Kha, and T. Q. Duong, "Practical optimization and game theory for 6G ultra-dense networks: Overview and research challenges," *IEEE Access*, vol. 10, pp. 13311–13328, 2022, doi: [10.1109/access.2022.3146335](https://doi.org/10.1109/access.2022.3146335).
- [11] E. Gelenbe and Y. Caseau, "The impact of information technology on energy consumption and carbon emissions," *Ubiquity*, vol. 2015, p. 115, Jun. 2015.
- [12] A. Andrae and T. Edler, "On global electricity usage of communication technology: Trends to 2030," *Challenges*, vol. 6, no. 1, pp. 117–157, Apr. 2015, doi: [10.3390/challe6010117](https://doi.org/10.3390/challe6010117).
- [13] (May 8, 2019). *Energy Efficiency: An Overview, Future Networks*. [Online]. Available: <https://www.gsma.com/futurenetworks/wiki/energy-efficiency-2/>
- [14] A. Srivastava, M. S. Gupta, and G. Kaur, "Energy efficient transmission trends towards future green cognitive radio networks (5G): Progress, taxonomy and open challenges," *J. Netw. Comput. Appl.*, vol. 168, Oct. 2020, Art. no. 102760.
- [15] L. Suarez, L. Nuaymi, and J.-M. Bonnin, "An overview and classification of research approaches in green wireless networks," *EURASIP J. Wireless Commun. Netw.*, vol. 2012, no. 1, pp. 1–18, Apr. 2012, doi: [10.1186/1687-1499-2012-142](https://doi.org/10.1186/1687-1499-2012-142).
- [16] S. Buzzi, C.-L. I, T. E. Klein, H. V. Poor, C. Yang, and A. Zappone, "Survey of energy-efficient techniques for 5G networks and challenges ahead," *IEEE J. Sel. Areas Commun.*, vol. 34, no. 4, pp. 697–709, Apr. 2016, doi: [10.1109/jsac.2016.2550338](https://doi.org/10.1109/jsac.2016.2550338).
- [17] M. Feng, S. Mao, and T. Jiang, "Base station on-off switching in 5G wireless networks: Approaches and challenges," *IEEE Wireless Commun.*, vol. 24, no. 4, pp. 46–54, Aug. 2017, doi: [10.1109/mwc.2017.1600353](https://doi.org/10.1109/mwc.2017.1600353).
- [18] Devopedia. (2022). *Dual Connectivity, Version 4*. Accessed: May 2, 2023. [Online]. Available: <https://devopedia.org/dual-connectivity>
- [19] Techplayon. (Jun. 14, 2019). *Dual Connectivity (DC) Definition, Protocol Architecture, DC and CA Comparison—Techplayon*. [Online]. Available: <http://www.techplayon.com/dual-connectivity-dc-definition-protocol-and-network-architecture-dc-and-ca-comparison/>.
- [20] B. Li, Y. Dai, Z. Dong, E. Panayirci, H. Jiang, and H. Jiang, "Energy-efficient resources allocation with millimeter-wave massive MIMO in ultra dense HetNets by SWIPT and CoMP," *IEEE Trans. Wireless Commun.*, vol. 20, no. 7, pp. 4435–4451, Jul. 2021, doi: [10.1109/twc.2021.3058776](https://doi.org/10.1109/twc.2021.3058776).
- [21] F. Fang, G. Ye, H. Zhang, J. Cheng, and V. C. M. Leung, "Energy-efficient joint user association and power allocation in a heterogeneous network," *IEEE Trans. Wireless Commun.*, vol. 19, no. 11, pp. 7008–7020, Nov. 2020, doi: [10.1109/twc.2020.2996628](https://doi.org/10.1109/twc.2020.2996628).
- [22] T. Van Chien, E. Björnson, and E. G. Larsson, "Joint power allocation and user association optimization for massive MIMO systems," *IEEE Trans. Wireless Commun.*, vol. 15, no. 9, pp. 6384–6399, Sep. 2016.
- [23] B. Zhuang, D. Guo, and M. L. Honig, "Energy-efficient cell activation, user association, and spectrum allocation in heterogeneous networks," *IEEE J. Sel. Areas Commun.*, vol. 34, no. 4, pp. 823–831, Apr. 2016.
- [24] K. Hammad, A. Moubayed, S. L. Primak, and A. Shami, "QoS-aware energy and jitter-efficient downlink predictive scheduler for heterogeneous traffic LTE networks," *IEEE Trans. Mobile Comput.*, vol. 17, no. 6, pp. 1411–1428, Jun. 2018.
- [25] Z. Si, G. Chuai, K. Zhang, W. Gao, X. Chen, and X. Liu, "Backhaul capacity-limited joint user association and power allocation scheme in ultra-dense millimeter-wave networks," *Entropy*, vol. 25, no. 3, p. 409, Feb. 2023, doi: [10.3390/e25030409](https://doi.org/10.3390/e25030409).
- [26] G. P. Koudouridis, H. Gao, and P. Legg, "A centralised approach to power on-off optimisation for heterogeneous networks," in *Proc. IEEE Veh. Technol. Conf. (VTC Fall)*, Sep. 2012, pp. 1–5.
- [27] J. Gao, Q. Ren, P. S. Gu, and X. Song, "User association and small-cell base station on/off strategies for energy efficiency of ultradense networks," *Mobile Inf. Syst.*, vol. 2019, p. 112, Jul. 2019, doi: [10.1155/2019/6871378](https://doi.org/10.1155/2019/6871378).
- [28] X. Huang, S. Tang, Q. Zheng, D. Zhang, and Q. Chen, "Dynamic femtocell gNB on/off strategies and seamless dual connectivity in 5G heterogeneous cellular networks," *IEEE Access*, vol. 6, pp. 21359–21368, 2018, doi: [10.1109/access.2018.2796126](https://doi.org/10.1109/access.2018.2796126).
- [29] N. Lassoued, N. Boujnah, and R. Bouallegue, "Reducing power consumption in C-RAN using switch on/off of MC-RRH sectors and small cells," *IEEE Access*, vol. 9, pp. 75668–75682, 2021, doi: [10.1109/access.2021.3081690](https://doi.org/10.1109/access.2021.3081690).
- [30] G. Femenias, N. Lassoued, and F. Riera-Palou, "Access point switch on/off strategies for green cell-free massive MIMO networking," *IEEE Access*, vol. 8, pp. 21788–21803, 2020, doi: [10.1109/access.2020.2969815](https://doi.org/10.1109/access.2020.2969815).
- [31] E. Oh, K. Son, and B. Krishnamachari, "Dynamic base station switching-on/off strategies for green cellular networks," *IEEE Trans. Wireless Commun.*, vol. 12, no. 5, pp. 2126–2136, May 2013, doi: [10.1109/twc.2013.032013.120494](https://doi.org/10.1109/twc.2013.032013.120494).
- [32] X. Lin, and S. Wang, "Joint user association and base station switching on/off for green heterogeneous cellular networks," in *Proc. IEEE Int. Conf. Commun. (ICC)*, May 2017, pp. 1–6.



- [33] Y. Zhu and S. Wang, "Joint traffic prediction and base station sleeping for energy saving in cellular networks," in *Proc. IEEE Int. Conf. Commun. (ICC)*, Jun. 2021, pp. 1–6.
- [34] A. Chen, S. Li, J. Xiong, K. Jin, and Z. Tang, "Joint user association and power allocation in ultra-dense mmWave networks: A multi-connectivity approach," 2022, *arXiv:2202.04070*.
- [35] W. Yu, H. Xu, A. Hematian, D. Griffith, and N. Golmie, "Towards energy efficiency in ultra dense networks," in *Proc. IEEE 35th Int. Perform. Comput. Commun. Conf. (IPCCC)*, Dec. 2016, pp. 1–8.
- [36] K. Venkateswararao and P. Swain, "Binary-PSO-based energy-efficient small cell deployment in 5G ultra-dense network," *J. Supercomputing*, vol. 78, no. 1, pp. 1071–1092, Jun. 2021, doi: [10.1007/s11227-021-03910-5](https://doi.org/10.1007/s11227-021-03910-5).
- [37] H. Zhang, S. Huang, C. Jiang, K. Long, V. C. M. Leung, and H. V. Poor, "Energy efficient user association and power allocation in millimeter-wave-based ultra dense networks with energy harvesting base stations," *IEEE J. Sel. Areas Commun.*, vol. 35, no. 9, pp. 1936–1947, Sep. 2017, doi: [10.1109/jsac.2017.2720898](https://doi.org/10.1109/jsac.2017.2720898).
- [38] Á. Ladányi and T. Cinkler, "Resilience–throughput–power trade-off in future 5G photonic networks," *Photonic Netw. Commun.*, vol. 37, no. 3, pp. 296–310, Mar. 2019, doi: [10.1007/s11107-019-00842-2](https://doi.org/10.1007/s11107-019-00842-2).
- [39] M. Jafri, A. Anand, S. Srivastava, A. K. Jagannatham, and L. Hanzo, "Robust distributed hybrid beamforming in coordinated multi-user multi-cell mmWave MIMO systems relying on imperfect CSI," *IEEE Trans. Commun.*, vol. 70, no. 12, pp. 8123–8137, Dec. 2022.
- [40] T. S. Rappaport, G. R. MacCartney, M. K. Samimi, and S. Sun, "Wideband millimeter-wave propagation measurements and channel models for future wireless communication system design," *IEEE Trans. Commun.*, vol. 63, no. 9, pp. 3029–3056, Sep. 2015, doi: [10.1109/tcomm.2015.2434384](https://doi.org/10.1109/tcomm.2015.2434384).
- [41] T. Camp, J. Boleng, and V. Davies, "A survey of mobility models for ad hoc network research," *Wireless Commun. Mobile Comput.*, vol. 2, no. 5, pp. 483–502, 2002, doi: [10.1002/wcm.72](https://doi.org/10.1002/wcm.72).
- [42] A. Jahid, M. H. Alsharif, P. Uthansakul, J. Nebhen, and A. A. Aly, "Energy efficient throughput aware traffic load balancing in green cellular networks," *IEEE Access*, vol. 9, pp. 90587–90602, 2021, doi: [10.1109/access.2021.3091499](https://doi.org/10.1109/access.2021.3091499).
- [43] T. H. Cormen, C. E. Leiserson, R. L. Rivest, and C. Stein, *Introduction to Algorithms*. Cambridge, MA, USA: MIT Press, 2001.
- [44] A. M. Hamed and R. K. Rao, "Evaluation of capacity and power efficiency in millimeter-wave bands," in *Proc. Int. Symp. Perform. Eval. Comput. Telecommun. Syst. (SPECTS)*, Jul. 2016, pp. 1–6.



**ABDULHALIM FAYAD** (Graduate Student Member, IEEE) received the B.S. degree in electronics and communication engineering and the M.S. degree in advanced communication engineering from Damascus University, Damascus, Syria, in 2014 and 2019, respectively. He is currently pursuing the Ph.D. degree with the HSN Laboratory, Department of Telecommunications and Media Informatics, Budapest University of Technology and Economics, Hungary. His main research interests include optical access networks, designing cost- and energy-efficient fronthaul architectures for 5G/6G networks, and resource allocation for 5G and beyond mmwave wireless networks.



**TIBOR CINKLER** received the M.Sc. and Ph.D. degrees from the Budapest University of Technology and Economics (BME), Hungary, in 1994 and 1999, respectively, and the joint Habilitation and D.Sc. degrees from the Hungarian Academy of Sciences, in 2013. He is currently a Full Professor with the Department of Telecommunications and Media Informatics (TMIT), BME. He is the author of over 300 refereed scientific publications, including four patents, with over 2600 citations.

His research interests include the optimization of communications networks, including optical networks, fronthaul/backhaul design for 5G/6G, and the IoT and 5G/5-based IIoT networks.



**JACEK RAK** (Senior Member, IEEE) received the M.Sc., Ph.D., and D.Sc. (Habilitation) degrees from the Gdańsk University of Technology, Gdańsk, Poland, in 2003, 2009, and 2016, respectively. He is currently the Head of the Department of Computer Communications, Gdańsk University of Technology. From 2016 to 2020, he was leading the COST CA15127 Action Resilient Communication Services Protecting End-User Applications From Disaster-Based Failures (RECODIS),

involving over 170 members from 31 countries. He has authored over 100 publications, including the book *Resilient Routing in Communication Networks* (Springer, 2015). His main research interests include the resilience of communication networks and networked systems. He was the TPC Chair of ONDM 2017 and the TPC Co-Chair of IFIP Networking 2019. He is a member of the editorial board of *Optical Switching and Networking* (Elsevier) and *Networks* (Wiley) and the Founder of the International Workshop on Resilient Networks Design and Modeling (RNDM).

...